Optical Materials 94 (2019) 130–137

Contents lists available at ScienceDirect

Optical Materials

journal homepage: www.elsevier.com/locate/optmat

Photocatalytic performance of TiO_2 thin film decorated with Cu_2O nanoparticles by laser ablation

Cao Deng[a], Ruijin Hong[a,b,*], Ming Jing[a], Jingqi Shi[a], Tingzhen Yan[a], Chunxian Tao[a], Dawei Zhang[a]

[a] Engineering Research Center of Optical Instrument and System, Ministry of Education and Shanghai Key Lab of Modern Optical System, University of Shanghai for Science and Technology, No.516 Jungong Road, Shanghai, 200093, People's Republic of China
[b] State Key Laboratory of Applied Optics, Changchun Institute of Optics, Fine Mechanics and Physics, Chinese Academy of Sciences, Changchun, 130033, China

ARTICLE INFO

Keywords:
TiO_2 thin film
Cu_2O nanoparticles
Laser ablation
Heterojunction
Photocatalytic performance

ABSTRACT

Cu_2O nanoparticles decorated TiO_2 thin films were fabricated by laser ablation. The effects of Cu_2O nanoparticles on the structure, optical properties and photocatalytic performance of TiO_2 thin film were investigated by X-ray diffraction (XRD), scanning electron microscope (SEM), X-ray photoelectron spectroscopy (XPS), Raman spectrometer system, optical absorption and photocatalytic evaluation system, respectively. XRD patterns indicate that the decoration has the effect of lowering the grain orientation of Cu_2O. The photocatalytic performance in hydrogen generation of Cu_2O decorated TiO_2 composite thin film was significantly improved compared with that of either Cu_2O nanoparticles or TiO_2 single layer thin film with 1.70 and 1.77 times, respectively. The oxidation of Cu_2O was demonstrated to dominate the photocatalytic performances of Cu_2O/TiO_2 composite thin films by varying the laser ablation powers.

1. Introduction

Hydrogen is considered as an important energy source for sustainable development due to its recyclability, safety and sustainability. In the early 1970s, Honda and Fujishima [1] reported that hydrogen was induced on the titanium dioxide (TiO_2) electrode by UV light. Since then, the photocatalytic application of TiO_2 has been studying extensively in water splitting [2,3]. However, pristine TiO_2 transmits only a partial solar energy to new energy due to the forbidden bandwidth of about 3.2 eV [4]. Many strategies have been developed to improve its photocatalytic performance [5]. But the photocatalytic activity was still limited by the recombination of internal carriers in TiO_2. Recently, the heterojunction between TiO_2 and the narrow gap semiconductor (such as ZnO, Cu_2O and MoS_2) [6–8], which benefits for the separation of carriers, draws lots of attentions. As a common p-type semiconductor with a band gap of approximately 2 eV [9], cuprous oxide (Cu_2O) not only has the characteristics of low cost and considerable activities, but also forms a heterojunction with TiO_2 easily [10,11]. For example, Xi et al. [12] prepared Cu_2O/TiO_2 nanoparticles by the solvothermal method, resulting in an increasing rate of hydrogen precipitation under simulated solar radiation. Xiang et al. [13] has published the deposition of Cu_2O nanoparticles on the TiO_2 nanotube array and showed the enhancement of its photodegradation activity. However, nanoparticles have limited its commercial applications, because they are prone to aggregate and difficult to separate and restore from solution [14]. Then, some studies put forward the idea of thin film for solving the previous problem due to their controllable particle size and immobile semiconductor nanoparticles [15,16]. But thin film has a relatively flat surface structure, resulting in a very small contact area between photocatalysts and reactant. Therefore, it is an urgent need to provide a method which can solve the above problems.

Laser ablation, which was carried out in vacuum, gaseous or liquid environment, has been developed for the synthesis of nanostructures [17–19]. Gondal et al. [20] performed the method of laser ablation in water to synthesize nanostructured Cu_2O by a Nd:YAG pulsed laser (operating at 532 nm wavelength with a pulse duration of 5 ns and a frequency of 10 Hz). Jung et al. [21] successfully prepared Cu, Cu_2O and CuO nanoparticles in different concentrations of NaOH solution by a simple technical laser ablation. As above, it can be seen that the high purity nanoparticles were prepared by laser ablation. On this basis, laser ablation in the atmosphere was conceived to prepare the nanoparticle film. In this method, ions ablated from the target are adhered to the substrate directly; thereby, the expectation that the sample has a nanoparticle structure, which separates from the solution easily and has

* Corresponding author.
E-mail address: rjhong@usst.edu.cn (R. Hong).

https://doi.org/10.1016/j.optmat.2019.05.030
Received 6 December 2018; Received in revised form 13 May 2019; Accepted 17 May 2019

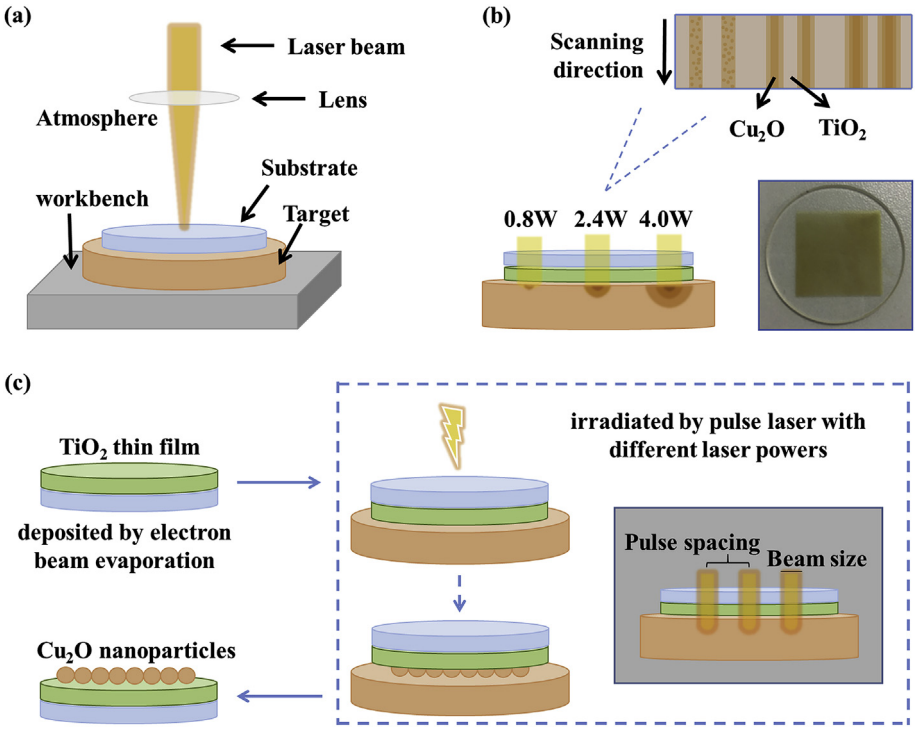

Fig. 1. Schematic diagrams of (a) nanoparticles growth by laser ablation, (b) the effect of laser beam power and (c) the preparation for Cu_2O nanoparticles decorated TiO_2 thin film.

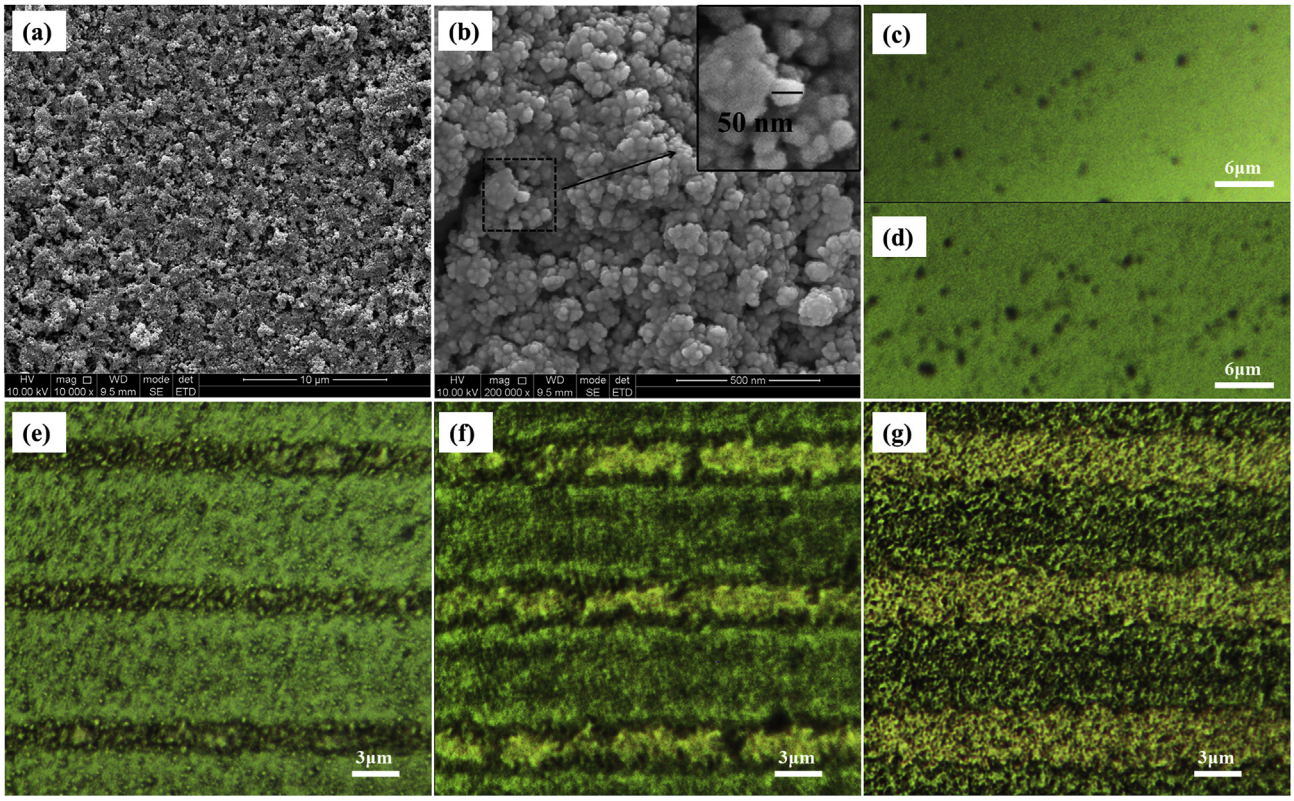

Fig. 2. SEM images of Cu_2O with the scale of (a) 10 μm and (b) 500 nm. (c)–(g) Optical microscope images of samples with the laser power of 0.8, 1.6, 2.4, 3.2 and 4.0 W.

a large contact area for participating in the photocatalytic reaction, can be successfully implemented.

In this paper, we propose a cost-effective technique for the nanofabrication of efficient decorating TiO_2 thin film with Cu_2O nanoparticles by a fairly simple laser ablation procedure. The photocatalytic performance of Cu_2O/TiO_2 composite thin films was enhanced and easily tuned by changing the laser power. The effects of Cu_2O nanoparticles decoration layer on structure, optical absorption and

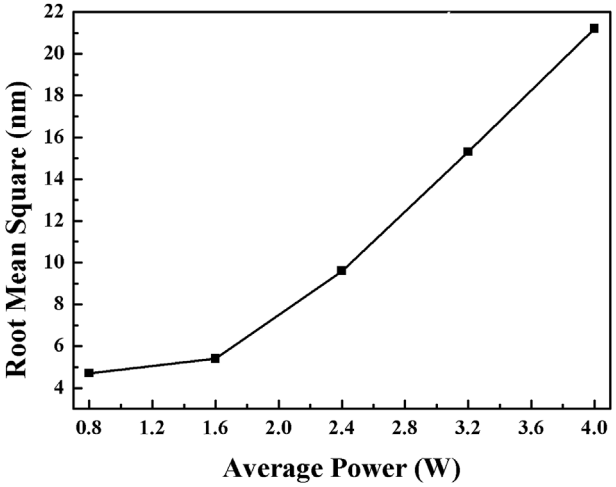

Fig. 3. RMS values of Cu_2O/TiO_2 composite thin films with different laser powers.

photocatalytic activity of TiO_2 thin film were investigated.

2. Experimental

Fig. 1(a) shows the schematic diagram of fabrication, a target was ablated by a neodymium-doped yttrium aluminium garnet (Nd:YAG) pulsed laser (the wavelength is 1064 nm and the maximum laser power is 20 W) under ambient conditions. TiO_2 thin films were deposited on k9 quartz glass by electron beam evaporation at the temperature of 200 °C. The thickness (about 100 nm) of TiO_2 thin film was monitored by a quartz crystal microbalance. Cu_2O layers were grown by laser ablation using a Cu_2O target (99.9%). The laser parameters adopted in the experiment were as follows: laser beam powers were set as 0.8, 1.6, 2.4, 3.2 and 4.0 W, respectively. The focal length, scanning rate, pulse width and line spacing of laser beam was 7.8 cm, 1000 mm/s, 4ns and 0.01 mm, respectively. The schematic of Cu_2O nanoparticles decorated TiO_2 thin film was shown in Fig. 1(c). The samples were marked as Sample1 (S1), Sample2 (S2), Sample3 (S3), Sample4 (S4) and Sample (S5), respectively, which are in accord with the increase of laser power.

The surface morphology was characterized by scanning electron microscope (SEM) (S-4800, Hitachi) and optical microscope. The surface roughness was measured by a step profiler (Ambios, XP-1). The crystal structures of samples were analyzed by X-ray diffraction (XRD) using a Rigaku MiniFlex600 system, with CuKα radiation (λ = 0.15408 nm). Raman scattering spectra were examined using a confocal microprobe Raman system (inVia Raman Microscope, Renishaw) with 633 nm laser. The optical absorption spectrum of samples was performed by using an UV-VIS-NIR double beam spectrophotometer (Lambda 1050, Perkins Elmer). Thermo Scientific K-Alpha + was used to study on the XPS.

Water splitting was carried out in a glass gas-closed-circulation system (CEL-SPH2N, Beijing) under irradiation with a 300 W xenon lamp (CEL-HXF 300). Typically, the sample was placed in a solution consisting of 50 mL deionized water. Then the air was sealed by rubber diaphragm. Prior to irradiation, the air and dissolved oxygen in the reaction mixture were removed by a vacuum pump. A cooling-water jacket was used to keep the photocatalytic reaction temperature at 6 °C. The deionized water with the photocatalyst was irradiated from the top using a 300 W xenon lamp jointing a cutoff filter to obtain UV-light irradiation. The photocatalytic activity was analyzed by extracting a certain amount of gas and employing N_2 carrying gas into a TCD gas

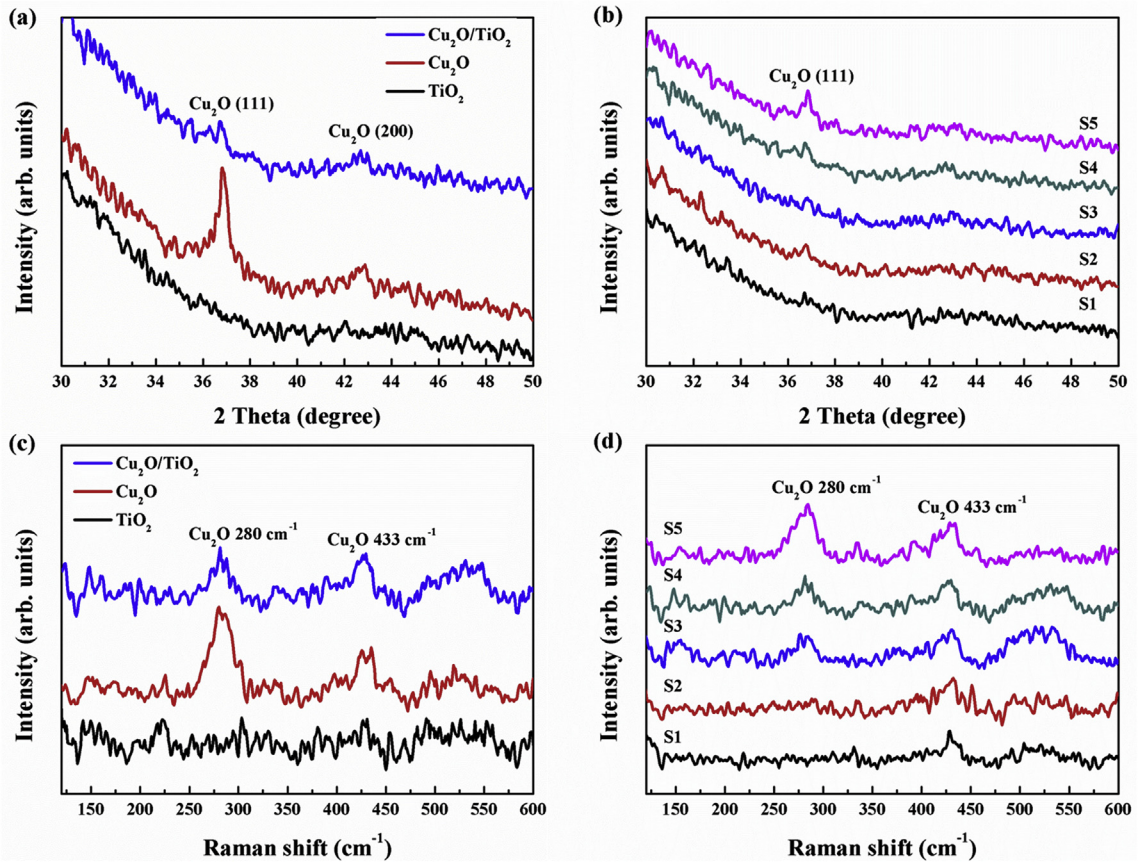

Fig. 4. XRD patterns of (a) Cu_2O, TiO_2, Cu_2O/TiO_2 composite thin film and (b) Cu_2O/TiO_2 composite samples with different laser powers. Raman spectra of (c) Cu_2O, TiO_2, Cu_2O/TiO_2 composite thin film and (d) Cu_2O/TiO_2 composite samples with different laser powers.

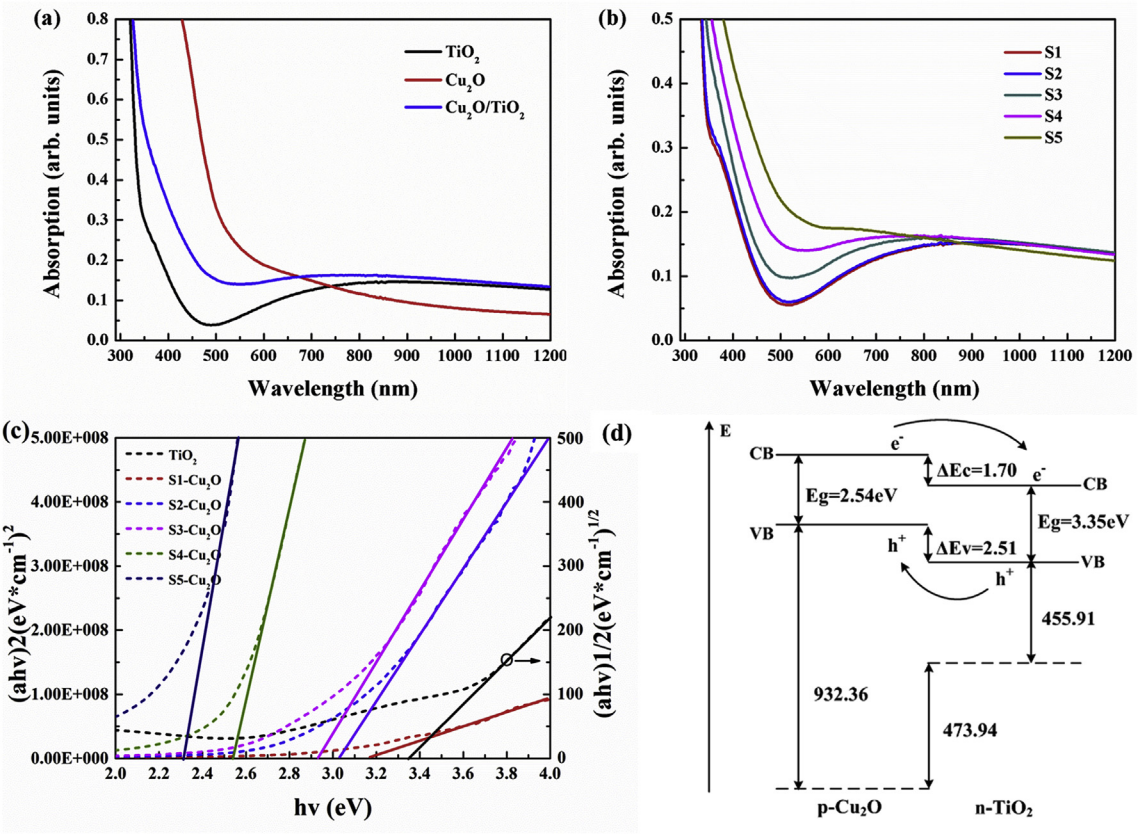

Fig. 5. Absorption spectra of (a) Cu_2O, TiO_2, Cu_2O/TiO_2 composite thin film and (b) Cu_2O/TiO_2 composite samples with different laser powers. (c) Optical band gap energy (Eg) of Cu_2O and TiO_2. (d) Schematic energy diagram of Cu_2O and TiO_2.

chromatograph equipped every half an hour.

3. Results and discussion

3.1. Surface morphology

Fig. 2(a) and (b) show the SEM images of Cu_2O nanoparticles decorated TiO_2 thin films with various magnifications. According to those images, the surface morphology of decoration layer is rough and porous, and a large number of nanoparticles with average diameter of approximately 50 nm accumulate tightly together. It means that the decoration layer prepared by laser ablation is consisted of small nanoparticles with large-size pores. In addition, a macro surface observation was also applied to samples with different laser powers by optical microscope with a 50 × objective lens, as shown in Fig. 2(c)-(g). The nanoparticles were distributed in a disordered state ablated with a low laser power, and then gradually aggregated on the scanning path of laser beam with wider scanning due to thermal effect with the increase of laser power.

Fig. 3 shows the root mean square (RMS) values of Cu_2O/TiO_2 composited thin films with the scanning area of 3 μm × 3 μm. With laser power increasing, the roughness of composite thin film increased. The RMS surface roughness values of these samples are 4.7, 5.4, 9.6, 15.3 and 21.2 nm, respectively.

In the case of laser ablation, the energy of photon is transferred to the electrons in the manner, causing a temperature rise. Then, the ions are gradually obtained the energy of electrons by electron-phonon coupling. When the thermal energy of ions is sufficient, the material melts to form the plasma and diffuses into the free space [22]. Therefore, with the laser power increasing, the quantity of energized electrons increases [23], resulting in a broader range of nanoparticles being ablated and attached to the substrate (as shown in Fig. 1(b)). Meanwhile, the heating of target in various locations is different by pulse laser (isothermal expansion occurs during the pulse and adiabatic expansion occurs after the pulse) [22], so the sample has a large number of pores. It is beneficial to increase the contact area of photocatalysts with reactant in the photocatalytic reaction.

3.2. Structural properties

XRD patterns as shown in Fig. 4(a) reveal the influence of laser ablation on the structure of Cu_2O and TiO_2. No diffraction peak is observed in TiO_2 thin film sample, indicating that it is amorphous phase. While it is apparent that Cu_2O deposited on glass substrate by laser ablation under ambient conditions is consisted of two diffraction peaks at around 36.48° and 42.41°, which correspond to the (111) and (200) peaks of Cu_2O, respectively (JCPDS 56–3288). The strong intensity of (111) diffraction peak indicates a preferred orientation of Cu_2O nanoparticles along the (111) crystallographic direction. No diffraction from randomly oriented grains or impurity phases is observed from the XRD spectrum. However, the XRD intensity of Cu_2O in composite thin film decreases drastically than that of single layer sample. Both the coupling and rough surface (compared with blank glass surface) of TiO_2 thin film contributed to degrade the diffraction or orientation in intensity. The diffraction peak of Cu_2O in composite samples increased in intensity with the laser power increasing (as shown in Fig. 4(b)).

Raman spectroscopy was also used to evaluate the crystalline quality. According to Fig. 4(c), no obvious Raman scattering peaks are detected in TiO_2 thin film. While two strong Raman bands at about 280 and 433 cm^{-1} are observed in Cu_2O nanoparticles, typically assigned to the structures of $2\Gamma_{12}^- + \Gamma_{25}^-$ and $4\Gamma_{12}^-$ in the silent modes of Cu_2O, respectively [24,25]. Where Γ_{12}^- corresponds to the twisting of Cu^+ tetrahedron around an axis (the two edges perpendicular to the axis rotating in opposite directions), and Γ_{25}^- corresponds to the opposite

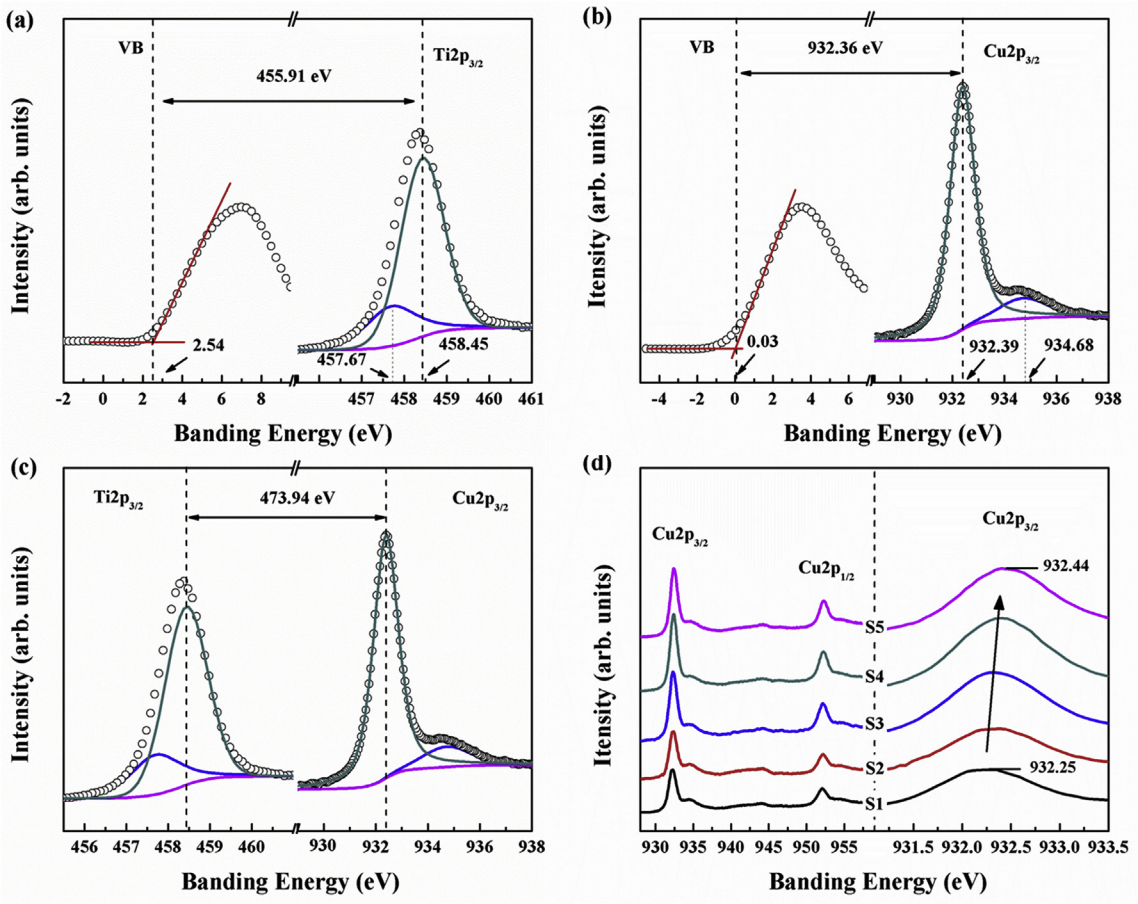

Fig. 6. XPS core-level and valence band spectra obtained from (a) TiO_2, (b) Cu_2O and (c) Cu_2O/TiO_2 composite thin film (d) Cu_2O/TiO_2 composite samples with different laser powers.

displacements of two $O^=$ lattices [25]. In the Cu_2O/TiO_2 composite sample, two Raman peaks are still observed with the weak intensity. But the intensity ratio of these two peaks is different from that of the single layer structure. The O element in the voids of TiO_2 thin film that stimulates the peak intensity of 433 cm^{-1}, may be the reason. In addition, it can be seen that the laser power has an effect on the intensity of Raman peaks (as shown in Fig. 4(d)). The variation tendency in the Raman peak of samples was similar to that of XRD pattern, and the Raman scatting intensities of peaks were enhanced with the laser increasing. It has been confirmed that the crystal quality of Cu_2O nanoparticles is controlled by varying the laser power.

3.3. Optical absorption

Optical absorption is critical to characterize the activity of photocatalysts and reflects the ability of thin film to produce electron-hole pairs. Fig. 5(a) shows the absorption spectra of single layer and composite samples. It indicates that the absorption curves of both Cu_2O and TiO_2 are typical semiconductor oxides with the maximum absorption peaks near the bandgap edge. The absorption intensity of Cu_2O/TiO_2 composite increases and the bandgap shows a red-shift compared with those of TiO_2 single layer thin films. With the laser power increasing, both the increase in absorption intensity and red-shift of bandgap are observed in the curves of Cu_2O/TiO_2 composite thin films.

The optical band gap of Cu_2O and TiO_2 can be calculated from absorption by the Tauc plot (Formula 1).

$$(\alpha h\nu)^2 = k(h\nu - Eg) \text{ or } (\alpha h\nu)^{1/2} = k(h\nu - Eg) \quad (1)$$

where α is absorption coefficient, k is a constant, $h\nu$ is the photon energy, and Eg is the optical band gap, respectively [26]. In general, the spectrum is the linear combination of the spectra of both components (Formula 2).

$$\alpha(h\nu) = a{\cdot}\alpha_s(h\nu) + b{\cdot}\alpha_m(h\nu) \quad (2)$$

where a and b determine the contributions of the components, while $\alpha_s(h\nu)$ and $\alpha_m(h\nu)$ are the absorption coefficients of the semiconductor and modified martials [27]. Here, the TiO_2 is only a single layer film obtained by electron beam evaporation, which means that $\alpha_m(h\nu)$ is not present. So the bandgap energy of TiO_2 should be calculated directly by the Tauc formula. It can be seen from Fig. 5(c) that the band-gap of TiO_2 is 3.35 eV, which is similar to that obtained in the literature [26]. And the forbidden band widths of Cu_2O nanoparticles ablated with the laser power of 0.8, 1.6, 2.4, 3.2 and 4.0 W is about 3.17, 3.03, 2.92, 2.54 and 2.31 eV, respectively. The energy diagram of Cu_2O and TiO_2 in Fig. 5(d) shows the reason why the composite sample converts more light to new energy by decorating a layer of Cu_2O nanoparticles on TiO_2 thin film. The conduction band value of Cu_2O is more negative than that of TiO_2. In this case, the thermodynamic condition favors the transfer of electrons from Cu_2O to TiO_2 [28].

3.4. Composition and valence state

To further obtain the information about the chemical states of Cu_2O nanoparticles decorated TiO_2 thin film by laser ablation, XPS was employed to characterize those samples (as shown in Fig. 6). The dot chart is the raw data obtained from the XPS measurements. According to $Ti2p_{3/2}$ core-level spectrum, two peaks located at around 457.7 and 463.7 eV, corresponding to Ti_2O_3 and TiO_2, respectively, are observed

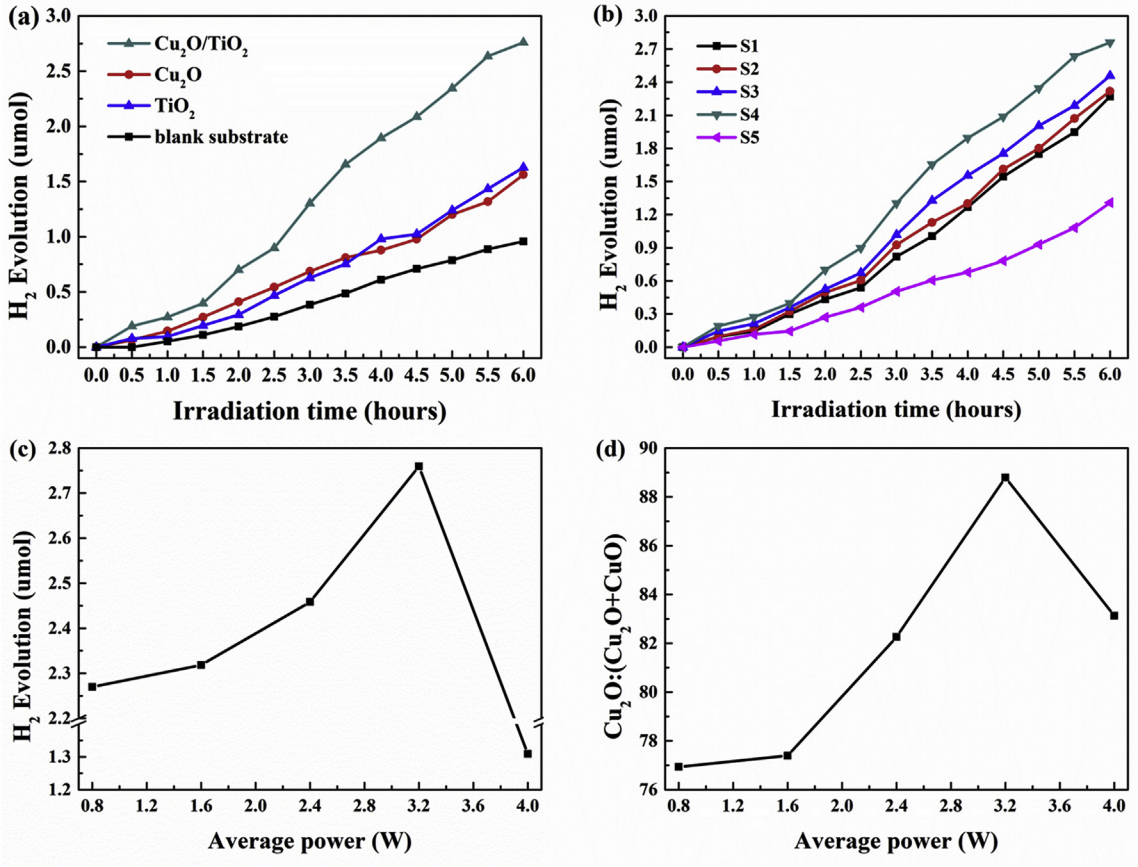

Fig. 7. The amount of H_2 produced by (a) blank substrate, Cu_2O, TiO_2, Cu_2O/TiO_2 composite thin film and (b) Cu_2O/TiO_2 composite samples with different laser powers in photocatalytic experiment under UV light irradiation. (c) Hydrogen yields of composite samples with different laser powers after 6 h UV irradiation. (d) Ratio of Cu_2O in decoration layers with different laser powers.

[29]. The appearance of Ti_2O_3 is due to insufficient oxygen in the chamber of coating machine during deposition. In addition, there are also two peaks located at around 932.3 and 934.6 eV in the $Cu2p_{3/2}$ core-level spectrum, corresponding to Cu_2O and CuO, respectively [30,31]. It indicates that the decoration layer obtained by laser ablation is principally consisted of Cu_2O with a small amount of CuO. So a peak-fit on the basis of deconvolution method was employed to find independent peaks related different valence states from the spectra (as shown in Fig. 6(d)). Those fitting results demonstrate that the composition of decoration layer is controlled by varying the laser power in the case of laser ablation.

With the laser power increasing, the ratio of Cu_2O in the decoration layer gradually increases, and then decreases with the further increase of laser power. Two separate processes could be concluded in the case of laser ablation (ablation process and decomposition process). With the laser power increasing, the photon energy from laser exerting to the Cu_2O target increases. The higher photon energy, the more Cu_2O particles are peeled off due to a sustained effect. This is referred to as ablation process. However, with the laser power further increasing, the surrounding temperature on target rises accordingly, which leads to an oxidation process of Cu_2O. The Cu_2O will be oxidized to CuO once the temperature is high enough [32]. Both of these two processes happened during laser ablation, and the rates of these two processes varied with the conditions, as shown in Fig. 7(d). In the case of laser power increased to 3.2 W, the ablation process kept a faster rate than the oxidation process. At the same time, the temperature of target also rose, resulting in an acceleration of oxidation (Cu_2O to CuO), as shown in the peak shift (Fig. 6(d)). When the laser power reached 4.0 W, the oxidation process was dominant, leading to a reduction of Cu_2O ratio in sample. Additionally, the nanoparticles amount of sample obtained by laser ablation with the laser power of 4.0 W increased (as shown in optical microscope images).

According to the XPS results, the method proposed by Kraut et al. [33] was employed to determine of the valence band offset at heterojunction interfaces. In this method, the valence band offset (ΔEv) and the conduction band offset (ΔEc) of heterojunction between Cu_2O and TiO_2 can be calculated. Fig. 6(a), (b) and (c) show the XPS core-level data of Cu_2O, TiO_2 and composite sample, respectively. Then, the data which obtained in the figures was taken into Formula 3-5 for calculation.

$$\Delta E_V = (E_{Cu,2p} - E_{V,Cu})_{Cu2O} - (E_{Ti,2p} - E_{V,Ti})_{TiO2} + \Delta E_{CL} \quad (3)$$

$$\Delta E_{CL} = (E_{Ti,2p} - E_{Cu,2p})_{Cu2O@TiO2} \quad (4)$$

$$\Delta E_C = E_{Cu2O} - E_{TiO2} + \Delta E_V \quad (5)$$

where, ΔEc is the main driving force for photoelectrons to transfer from Cu_2O to TiO_2 [34]. As shown in Fig. 5(d), the sample has a higher ΔEc value compared to Liu's work [35]. The result shows that Cu_2O nanoparticles decorated TiO_2 thin film has a large driving force, which is helpful to enhance the separation and transfer of charge.

3.5. Photocatalysis

The photocatalytic performances of all samples were measured by photocatalytic evaluation system under UV light irradiation. After 6 h irradiation, the hydrogen yields of Cu_2O and TiO_2 was 1.63 μmol and 1.56 μmol, respectively (Fig. 7(a)). While the hydrogen generation of TiO_2 thin film decorated with Cu_2O nanoparticles was 2.76 μmol, which was 1.77 times than that of TiO_2 single layer thin film. It indicates that

the photocatalytic performance of TiO_2 thin film has a great improvement with the decoration of Cu_2O nanoparticles. In general, the photocatalytic activity of Cu_2O is weaker than that of TiO_2 due to the large differences of band gap energy and the carrier recombination between Cu_2O and TiO_2 [28]. However, here the hydrogen yield of Cu_2O is almost equivalent to that of TiO_2. Because the decoration layer obtained by laser ablation is featured with porous, resulting in a larger contact surface for water splitting than that of thin film obtained by physical vacuum deposition. Additionally, the heterojunction formed between Cu_2O and TiO_2 provides a built-in electric field drive for electron-hole separation [16,36]. According to the calculation results of both the band gaps of single layer samples and the conduction band offsets of heterojunction, the photoelectrons (generated from the Cu_2O) are transferred to the TiO_2 because the CB of Cu_2O is lower than that of TiO_2. The internal recombination of electron-hole is successfully reduced and charge separation is accelerated because of the high driving force.

Reasonable control of laser power is also a key factor in the case of fabricating the Cu_2O nanoparticles decorated TiO_2 composite thin film. With the laser power increasing, the photocatalytic activity exhibits a significant difference, as shown in Fig. 7(b). And the variation tendency of hydrogen generation in composite samples is similar to that of Cu_2O ratios in the decoration layer (Fig. 7(c)). The hydrogen generation of composite samples was enhanced with the power increasing to 3.2 W. It should be attributed to that a high power laser beam is able to ablate more Cu_2O nanoparticles on the surface of TiO_2 thin film, leading to a wide range of heterojunctions. Moreover, the composite sample, fabricating with a higher laser power, has a better crystalline qualities of (100) and (111) crystal orientations on the decoration layer, which is beneficial to improve the photocatalytic efficiency [37–39]. Unfortunately, with the laser power further increasing, the photocatalytic performance of composite sample abruptly decreased due to a reduced proportion of Cu_2O and an increase of charge trapping mechanism [40,41].

4. Conclusion

In conclusion, the influence of decoration layer on the composition, morphology, crystal quality and optical properties of TiO_2 thin film were investigated in this paper. SEM and optical microscope images show that the decoration layer has a nanoparticle structure with pores, and both ratio and quantity of Cu_2O can be tuned by varying the laser power. The heterojunction between the Cu_2O nanoparticles and TiO_2 thin film leads to a significant improvement of absorption. The hydrogen generation of Cu_2O nanoparticles decorated TiO_2 thin film is 1.70 and 1.77 times than those of Cu_2O nanoparticles and TiO_2 single layer thin film under UV irradiation respectively, indicating that the photocatalytic efficiency is obviously enhanced.

Declaration of interest statement

We declare that we have no financial and personal relationships with other people or organizations that can inappropriately influence our work, there is no professional or other personal interest of any nature or kind in any product, service and/or company that could be construed as influencing the position presented in, or the review of, the manuscript entitled.

Acknowledgements

This work was partially supported by the National Natural Science Foundation of China (61775140, 61775141), Shanghai Foundation for Science and Technology Innovation Action Plan (15441902302, 1714220060) and the National Key Research and Development Program of China (2016YFB1102303).

References

[1] A. Fujishima, K. Honda, Electrochemical photolysis of water at a semiconductor electrode, Nature 238 (1972) 37–38.
[2] T. Tachikawa, M. Fujitsuka, T. Majima, Mechanistic insight into the TiO_2 photocatalytic reactions: design of new photocatalysts, J. Phys. Chem. C 111 (2007) 5259–5275.
[3] A. Fujishima, TiO_2 photocatalysis and related surface phenomena, Surf. Sci. Rep. 63 (2008) 515–582.
[4] Dette, M.A. Perez-Osorio, C.S. Kley, P. Punke, C.E. Patrick, P. Jacobson, F. Giustino, S.J. Jung, K. Kern, TiO_2 anatase with a bandgap in the visible region, Nano Lett. 14 (2014) 6533–6538.
[5] S. Chen, D. Li, Y. Liu, W. Huang, Morphology-dependent defect structures and photocatalytic performance of hydrogenated anatase TiO_2 nanocrystals, J. Catal. 341 (2016) 126–135.
[6] L. Xu, G. Zheng, H. Wua, J. Wang, F. Gu, J. Su, F. Xian, Z. Liu, Strong ultraviolet and violet emissions from ZnO/TiO_2 multilayer thin films, Opt. Mater. 35 (2013) 1582–1586.
[7] F. Zhao, Y. Rong, J. Wan, Z. Hua, Z. Peng, B. Wang, MoS_2 quantum dots@TiO_2 nanotube composites with enhanced photoexcited charges separation and high-efficiency visible-light driven photocatalysis, Nanotechnology 29 (2018) 105403.
[8] Q. Ding, S. Chen, F. Shang, J. Liang, C. Liu, Cu_2O/Ag co-deposited TiO_2 nanotube array film prepared by pulse-reversing voltage and photocatalytic properties, Nanotechnology 27 (2016) 485705.
[9] P.D. Jongh, D. Vanmaekelbergh, J.J. Kelly, Cu_2O: electrodeposition and characterization, Chem. Mater. 11 (2015) 3512–3517.
[10] S. Chatterjee, A.J. Pal, Introducing Cu_2O thin films as a hole-transport layer in efficient planar perovskite solar cell structures, J. Phys. Chem. C (2016) 120–1437 1428.
[11] S. Massidda, J. Yu, A.J. Freeman, Electronic structure and properties of $Bi_2Sr_2CaCu_2O_8$, the third high-Tc superconductor, Physica C 152 (2015) 251–258.
[12] Z. Xi, C. Li, L. Zhang, M. Xing, J. Zhang, Synergistic effect of Cu_2O/TiO_2 heterostructure nanoparticle and its high H_2 evolution activity, Int. J. Hydrogen Energy 39 (2014) 6345–6353.
[13] L.Y. Xiang, J. Ya, F.J. Hu, L.X. Li, Z.F. Liu, Fabrication of Cu_2O/TiO_2 nanotube arrays with enhanced visiblelight photoelectrocatalytic activity, Appl. Phys. A 123 (2017) 160.
[14] J. Dong, H. Xu, F. Zhang, C. Chen, L. Liu, G. Wu, Synergistic effect over photocatalytic active Cu_2O Thin films and their morphological and orientational transformation under visible light irradiation, Appl. Catal., A 470 (2014) 294–302.
[15] P. Swarnakar, S.R. Kanel, D. Nepal, Y. Jiang, H. Jia, L. Kerr, M.K. Goltz, J. Levy, J. Rakovan, Silver deposited titanium dioxide thin film for photocatalysis of organic compounds using natural light, Sol. Energy 88 (2013) 242–249.
[16] Y.G. Zhang, L.L. Ma, J.L. Li, Y. Yu, In situ Fenton reagent generated from TiO_2/Cu_2O composite film a new way to utilize TiO_2 under visible light irradiation, Environ. Sci. Technol. 41 (2007) 6264–6269.
[17] A.L. Schawlow, C.H. Townes, Infrared and optical masers, J. Am. Soc. Naval Eng. 73 (1961) 45–50.
[18] T.H. Maiman, Stimulated optical radiation in ruby, Nature 187 (1969) 134–136.
[19] A.M. Morales, C.M. Lieber, A laser ablation method for the synthesis of crystalline semiconductor nanowires, Science 279 (1998) 208–210.
[20] M.A. Gondal, T.F. Qahtan, M.A. Dastageer, Y.W. Maganda, D.H. Anjum, Synthesis of Cu/Cu_2O nanoparticles by laser ablation in deionized water and their annealing transformation into CuO nanoparticles, J. Nanosci. Nanotechnol. 13 (2013) 5759–5766.
[21] H.J. Jung, Y. Yu, M.Y. Choi, Facile preparation of Cu_2O and CuO nanoparticles by pulsed laser ablation in NaOH solutions of different concentration, Bull. Korean Chem. Soc. 36 (2015) 3–4.
[22] M. Hashida, H. Mishima, S. Tokita, S. Sakabe, Non-thermal ablation of expanded polytetrafluoroethylene with an intense femtosecond-pulse laser, Optic Express 17 (2009) 13116–13121.
[23] M. Jing, R. Hong, W. Shao, H. Lin, D. Zhang, S. Zhuang, D. Zhang, Laser induced photocatalytic activity enhancement of TiO_2 thin films, Optic Express 25 (2017) 1132–1138.
[24] H. Kung, The long wave modes of the Cu_2O lattice, Z. Angew. Phys. 171 (1963) 213–225.
[25] C. Carabatos, Lattice vibrations of Cu_2O at the long wave limit, Phys. Status Solidi 37 (1970) 773–779.
[26] M. Jing, R. Hong, W. Wei, C. Tao, D. Zhang, S. Zhuang, Difference of SERS ability from titanium oxide films by Ti_{3p} self-doping, Opt. Mater. 73 (2017) 371–376.
[27] P. Makuja, M. Pacia, W. Macyk, How to correctly determine the band gap energy of modified semiconductor photocatalysts based on UV−Vis spectra, J. Phys. Chem. Lett. 9 (2018) 6814–6817.
[28] J.Y. Zhang, H.L. Zhu, S.K. Zheng, F. Pan, T.M. Wang, TiO_2 film/Cu_2O microgrid heterojunction with photocatalytic activity under solar light irradiation, Acs Appl. Mat. Interfaces 1 (2009) 2111–2114.
[29] R. Castillo, B. Koch, P. Ruiz, B. Delmon, Influence of the amount of titania on the texture and structure of titania supported on silica, J. Catal. 161 (1996) 524–529.
[30] I. Nakai, Y. Sugitani, K. Nagashima, Y. Niwa, X-ray photoelectron spectroscopic study of copper minerals, J. Inorg. Nucl. Chem. 50 (1978) 789–791.
[31] F. Parmigiani, G. Pacchioni, F. Illasl, P.S. Bagus, Studies of the Cu-0 bond in cupric oxide by X-ray photoelectron spectroscopy and ab initio electronic structure models, J. Electron. Spectrosc. Relat. Phenom. 59 (1992) 255–269.
[32] S. Jamali, A. Moshaii, N. Mohammadian, Improvement of photoelectrochemical and stability properties of electrodeposited Cu_2O thin films by annealing processes,

Phys. Status Solidi 214 (2017) 1700380.
[33] E.A. Kraut, R.W. Grant, J.R. Waldrop, S.P. Kowalczyk, Semiconductor core-level to valence-band maximum binding-energy differences: precise determination by x-ray photoelectron spectroscopy, Phys. Rev. B 28 (1983) 1965–1977.
[34] B. Kramm, A. Laufer, D. Reppin, A. Kronenberger, P. Hering, A. Polity, B.K. Meyer, The band alignment of Cu_2O/ZnO and Cu_2O/GaN heterostructures, Appl. Phys. Lett. 100 (2012) 094102.
[35] L. Liu, W. Yang, W. Sun, Q. Li, J.K. Shang, Creation of Cu_2O@TiO_2 composite photocatalysts with p-n heterojunctions formed on exposed Cu_2O facets, their energy band alignment study, and their enhanced photocatalytic activity under visible light illumination, ACS Appl. Mater. Interfaces 7 (2015) 1465–1476.
[36] Y. Liu, B. Zhang, L. Luo, X. Chen, Z. Wang, E. Wu, D. Su, W. Huang, TiO_2/Cu_2O core/ultrathin shell nanorods as efficient and stable photocatalysts for water reduction, Angew. Chem. Int. Ed. 54 (2016) 15260–15265.
[37] H. Gao, J. Zhang, M. Li, K. Liu, D. Guo, Y. Zhang, Evaluating the electric property of different crystal faces and enhancing the Raman scattering of Cu_2O microcrystal by depositing Ag on the surface, Curr. Appl. Phys. 13 (2013) 935–939.
[38] J.Y. Ho, M.H. Huang, Synthesis of submicrometer-sized Cu_2O crystals with morphological evolution from cubic to hexapod structures and their comparative photocatalytic activity, J. Phys. Chem. C 113 (2009) 14159–14164.
[39] G. Wu, Q. Shen, H. Yu, T. Zhao, C. Lu, A. Liu, Reduced graphene oxide encapsulated Cu_2O with controlled crystallographic facets for enhanced visible-light photocatalytic degradation, Funct. Mater. Lett. 10 (2017) 1750034.
[40] Y. Bessekhouad, D. Robert, J.V. Weber, Photocatalytic activity of Cu_2O/TiO_2, Bi_2O_3/TiO_2 and $ZnMn_2O_4$/TiO_2 heterojunctions, Catal. Today 101 (2005) 315–321.
[41] Y. Liao, P. Deng, X. Wang, D. Zhang, F. Li, Q. Yang, H. Zhang, Z. Zhong, A facile method for preparation of Cu_2O-TiO_2 NTA heterojunction with visible-photocatalytic activity, Nanoscale Res. Lett. 13 (2018) 221.